Electronic Supplementary Information for Dalton Transactions

Supporting Information

Rationally Designed Chiral Ni_5L_6 Clusters with the in Situ Generated Tridentate Ligand. Hydrothermal Synthesis, Crystal Structures, Morphology and Magnetic Properties

Sisi Feng[a], *Miaoli Zhu*[*a,c], *Liping Lu*[*a], *Lei Du*[b], *Yunbo Zhang*[*b], *Tianwei Wang*[c]

Table S1a Hydrogen bond distances and angles (Ǻ and °) for complex ***5***

D-H...A	d(D-H)	d(H...A)	d(D...A)	<(DHA)
O(13)-H(13A)...O(14C)#1	0.92	2.32	3.08(3)	140.1
O(13)-H(13B)...O(10)	0.88	2.13	2.88(2)	142.0
O(12)-H(12B)...O(13)	0.72	2.53	3.13(2)	143.5
O(12)-H(12A)...O(11A)	0.87	2.36	3.090(15)	141.5
O(11A)-H(11A)...O(14B)#2	0.80	2.08	2.87(2)	168.5
O(10)-H(10A)...O(7)	0.74	2.59	3.317(12)	168.3
O(10)-H(10A)...O(8)	0.74	2.46	3.046(11)	137.1
N(22)-H(22)...O(14A)	0.88	2.17	3.04(2)	174.7
N(20)-H(20)...O(13)	0.88	2.13	2.950(16)	155.5
N(18)-H(18)...O(10)	0.88	2.08	2.939(11)	164.5
N(16)-H(16)...O(14C)#3	0.88	1.96	2.835(17)	169.6
N(14)-H(14)...O(14B)	0.88	1.98	2.847(19)	167.4
N(12)-H(12)...O(12)	0.88	2.04	2.883(13)	160.9
N(10)-H(10)...O(11A)	0.88	1.93	2.807(10)	173.4
N(8)-H(8)...O(14A)#3	0.88	2.23	2.95(2)	139.6
N(6)-H(6)...O(8)#4	0.88	2.00	2.874(8)	172.0
N(4)-H(4)...O(10)#5	0.88	2.02	2.900(9)	174.8
N(2)-H(2)...O(7)#5	0.88	2.00	2.871(8)	171.9

#1 -x+1,y+1/2,-z+1/2; #2 x,-y+1/2,z+1/2; #3 x+1,y,z; #4 -x+2,y-1/2,-z+1/2; #5 -x+1,y-1/2,-z+1/2

Table S1b Hydrogen bond distances and angles (Ǻ and °) for complex ***6***

D-H...A	d(D-H)	d(H...A)	d(D...A)	<(DHA)
N(2)-H(2)...Br(1)	0.88	2.39	3.241(5)	161.4
N(4)-H(4)...Br(4)#1	0.88	2.27	3.097(7)	157.2
N(6)-H(6)...Br(9)#2	0.88	1.99	2.866(13)	176.3
N(6)-H(6)...Br(8)#2	0.88	2.34	3.186(8)	161.0

N(8)-H(8)...Br(3)#3	0.88	2.38	3.254(7)	169.9
N(10)-H(10)...Br(7)#2	0.88	2.21	3.086(6)	173.7
N(12)-H(12)...Br(2)#2	0.88	2.61	3.320(9)	139.0
N(14)-H(14)...Br(10)#2	0.88	2.27	3.144(11)	169.5
N(16)-H(16)...Br(2)#2	0.88	2.79	3.529(7)	142.3
N(18)-H(18)...Br(2)	0.88	2.44	3.318(7)	174.6
N(20)-H(20)...Br(7)	0.88	2.44	3.166(7)	140.8
N(22)-H(22)...Br(4)	0.88	2.46	3.324(8)	166.7
N(24)-H(24)...Br(6)	0.88	2.25	3.059(12)	153.2

#1 -x+1,y+1/2,-z+1/2; #2 x-1,y,z; #3 x,-y+1/2,z-1/2

Table S1c Hydrogen bond distances and angles (Å and °) for complex *7*

D-H...A	d(D-H)	d(H...A)	d(D...A)	<(DHA)
N(24)-H(24)...I(1B)#1	0.88	3.08	3.488(9)	110.8
N(22)-H(22)...I(4A)#2	0.88	2.66	3.536(8)	174.9
N(20)-H(20)...I(4A)#3	0.88	2.82	3.564(11)	143.8
N(20)-H(20)...I(2A)#2	0.88	3.15	3.675(9)	120.7
N(20)-H(20)...I(2C)#2	0.88	3.16	3.71(3)	122.7
N(16)-H(16)...I(3C)	0.88	2.14	2.958(11)	153.3
N(14)-H(14)...I(3B)	0.88	2.17	3.018(13)	161.6
N(12)-H(12)...I(3A)	0.88	2.60	3.475(9)	171.5
N(12)-H(12)...I(3D)	0.88	2.03	2.85(2)	155.1
N(10)-H(10)...I(4C)	0.88	1.98	2.856(14)	170.3
N(10)-H(10)...I(4B)	0.88	2.64	3.432(7)	150.8
N(8)-H(8)...I(3B)#1	0.88	2.10	2.955(9)	165.0
N(6)-H(6)...I(1B)#1	0.88	2.86	3.697(5)	160.1
N(6)-H(6)...I(1A)#1	0.88	2.63	3.484(5)	163.4
N(4)-H(4)...I(4A)#3	0.88	2.89	3.596(8)	138.8
N(2)-H(2)...I(1B)#4	0.88	2.85	3.579(6)	141.7

#1 -x+1,y+1/2,-z+3/2; #2 x,-y+3/2,z+1/2; #3 x-1,-y+3/2,z+1/2; #4 -x,y+1/2,-z+3/2

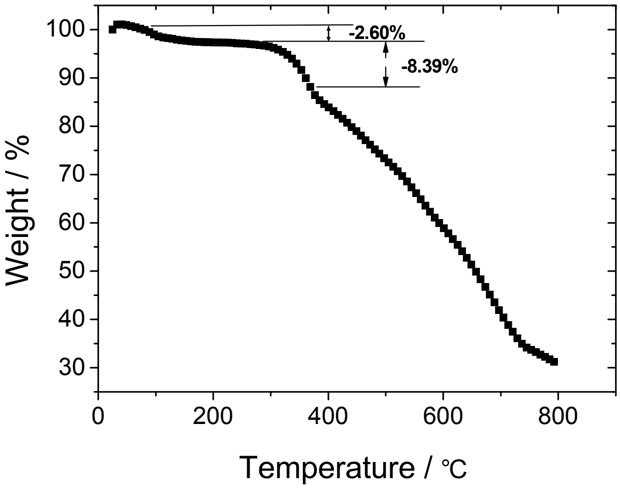

Figure S1. TG spectrum of complex ***5***.

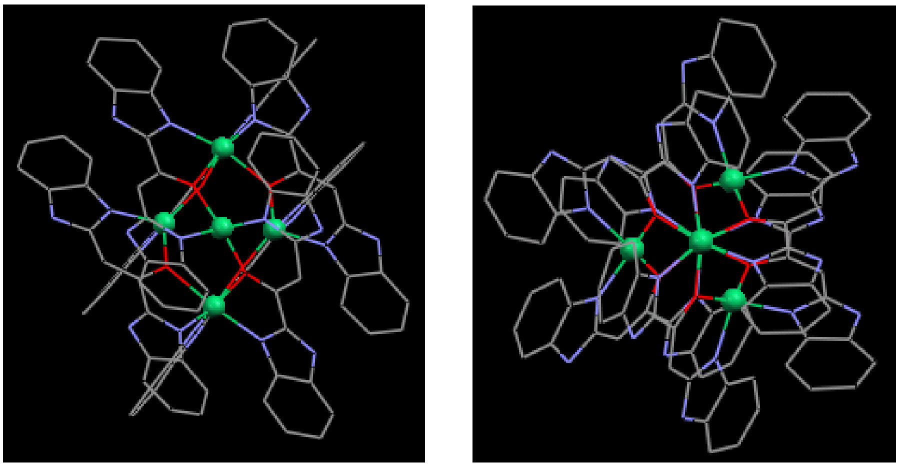

Figure S2 View of the cation of the molecular structure in ***5*** (left: view from the C_2 axis and right: view from the C_3 axis) with hydrogen atoms omitted for clarity. The green spheres represent Ni atoms and the wireframe represents the ligand with carbon atoms shown in gray, oxygen atoms in red and nitrogen atoms in blue.

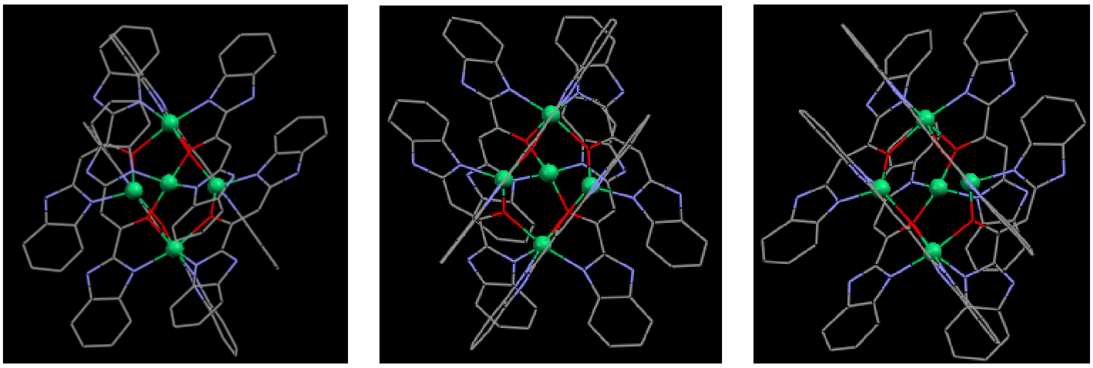

(a) (b) (c)

Figure S3 View of the cations of the molecular structures in ***4*** (a), ***6***(b) and *7*(c) with hydrogen atoms omitted for clarity. The green spheres represent Ni atoms, and the wireframe represents the ligand with carbon atoms shown in gray, oxygen atoms in red and nitrogen atoms in blue.

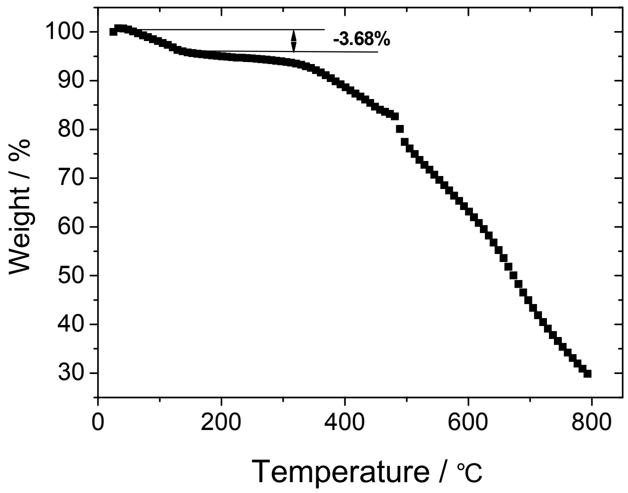

Figure S4. TG spectrum of complex ***2***, solvent and coordinated water molecules loss of 3.68% (calcd: 3.63%).

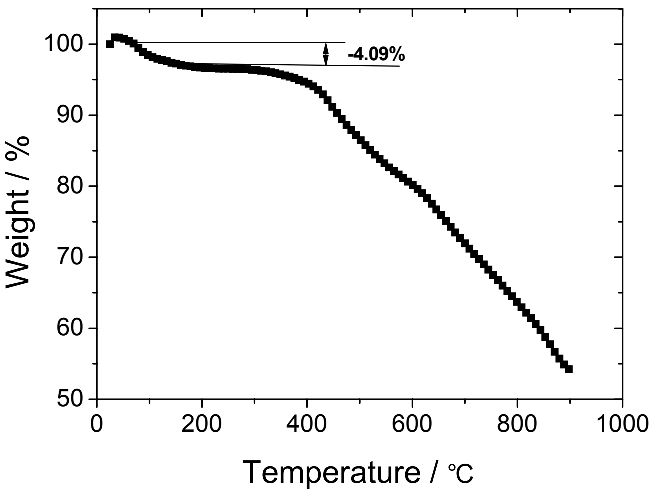

Figure S5. TG spectrum of complex ***3***, five water molecules lose of 4.09% below 350 °C (calcd: 4.13%).

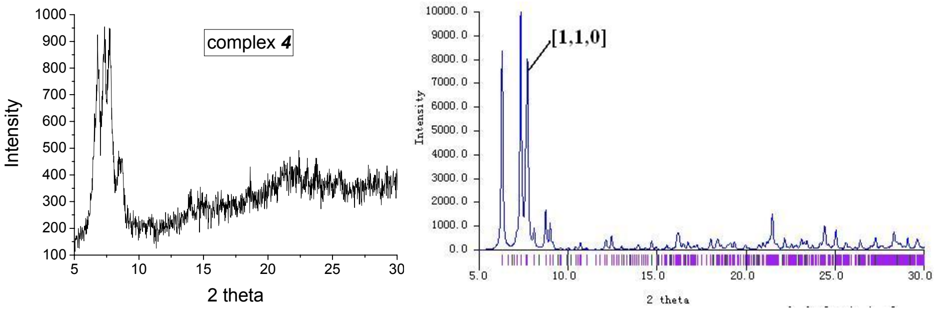

Figure S6. The XRPD patterns for complex ***4***. Left for experimental curves, right for simulated curves. XRPD patterns were measured at room temperature.

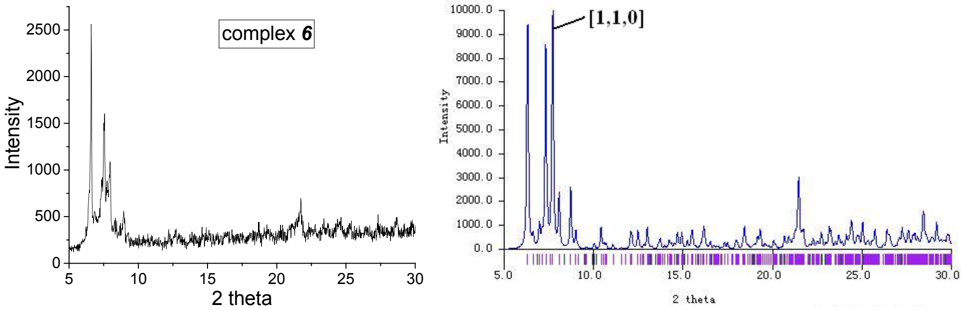

Figure S7. The XRPD patterns for complex ***6***. Left for experimental curves, right for simulated curves. XRPD patterns were measured at room temperature.

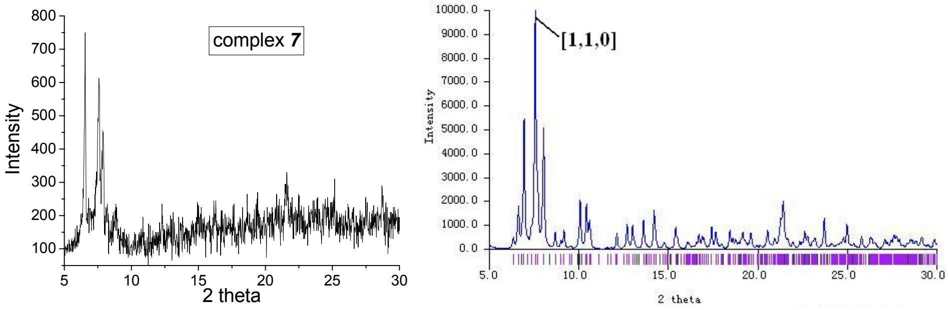

Figure S8. The XRPD patterns for complex *7*. Left for experimental curves, right for simulated curves. XRPD patterns were measured at room temperature.

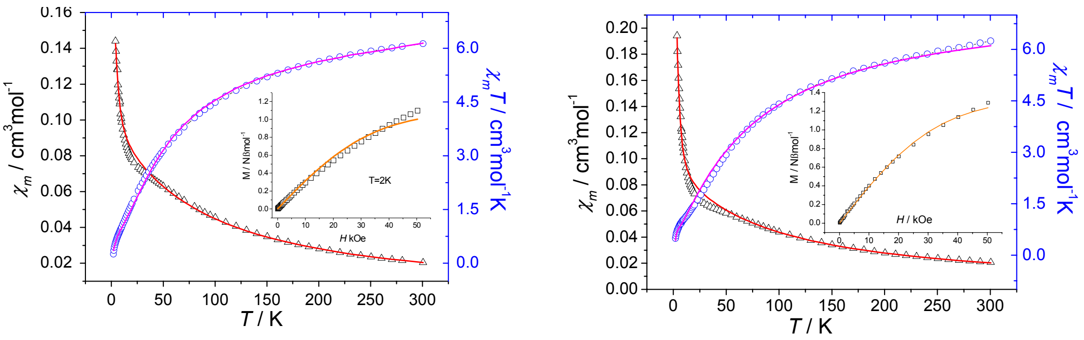

Figure S9. Magnetic susceptibility (χ_{mol}) (Δ) and its product with temperature ($\chi_m T$) (o) for compounds ***4*** (left) and *7* (right) as a function of temperature (applied field 1 KOe). The solid line (red line-χ_{mol} and magenta line-$\chi_m T$) represents the result of numerical calculation. Magnetic moment data (□) as a function of field are shown in the inset together with the Brillouin function(orange line)

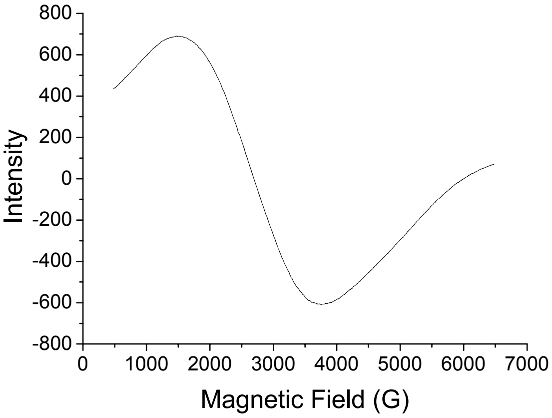

Figure S10. EPR spectra of crystal sample of complex ***4*** measured at 298 K in X-band (9.7737GHz)

Table S2 short ring – ring contacts in 5, 6, and 7

Ring-i	Ring-j	5	6	7
Cg1	Cg6	3.164(4)	3.180(3)	3.099(4)
Cg2	Cg3	3.100(4)	3.092(3)	3.186(3)
Cg3	Cg2	3.101(4)	3.184(3)	3.172(4)
Cg4	Cg5	3.237(4)	3.181(3)	3.099(4)
Cg5	Cg4	3.237(4)	3.093(3)	3.186(3)
Cg6	Cg1	3.163(4)	3.183(3)	3.172(4)

Cg1 for centre of ring Ni3/O1/C1/C9/C10/N3, Cg2 for Ni3/O4/C49/C57/C58/N15, Cg3 for Ni4/O2/C17/C25/C26/N7, Cg4 for Ni4/O5/C65/C73/C74/N19 , Cg5 for Ni5/O3/C33/C41/C42/N11, Cg6 for Ni5/O6/C81/C89/C90/N23

S.1 Comments on crystal structure refinements

Collected complete diffraction data with P1 space group of the three crystals for complexes 5, 6 and 7 at 120 K and resolved three structures from the data at low temperature. Diffaction data were well observed at high resolution with 97% completeness. The structural models of complexes 5, 6, and 7 were resolved following normal processes by programs SHELXTL[1] and PLATON[2]. H atoms attached to C and N atoms of all three complexes were placed in geometrically idealized positions, with Csp^2-H = 0.93, and Nsp^3-H = 0.86 Å and refined with $U_{iso}(H) = 1.2U_{eq}$(C or N). H atoms attached to O were located from difference Fourier maps and refined as riding in their as-found positions with $U_{iso}(H) = 1.5U_{eq}(O)$ for 100% occupancy and $U_{iso}(H) = 1.0U_{eq}(O)$ for partial occupancy. All structure solutions show the three complexes crystallized with monoclinic and $P2_1/c$ space group in the crystallography.

Complex 5, we design originally that the anions should be four NO_3^-, but only one NO_3^- was found in the process of refinement. So, three hydroxide anions in the solvent O atoms were considerable for charge balance. Frankly, assign of hydroxide anions were stochastic in these O atoms. There were disorder and partially occupied sites for the antiparticles, O11A and O11B as well as O14A, O14B and O14C. The occupancies of these sites were freely refined with PART and SUMP instruction. ISOR instruction was employed to have ellipsoids of sites (O14A, O14B, O14C and O11B) be restraint to more appropriate values. So, 25 restraints were used for refinement anisotropically.

Further, checkcif report indicated that the structure contains large solvent accessible voids of 950.6 $Å^3$/per unit cell, i.e. some 9.84% of the total volume. Data were corrected for disordered electron density through use of the SQUEEZE[2] procedure. Attempts to refine peaks of residual electron density as solvent O atoms (water) and NO3 anion were unsuccessful. Derived values (formula weight, density, absorption coefficient) do not contain the contribution of the disordered solvent molecule.

In 6, Fourier maps show that there were partial occupancies for all four Br^- ions. The occupancies of these sites were freely refined with PART and SUMP instruction firstly until convergence, and then fixed at final refine with partial occupancies for Br1 0.75, Br2 0.70, Br3 0.50, Br4 0.40, Br5 0.20, Br6 0.20, Br7 0.45, Br8 0.23, Br9 0.22, Br10 0.20, Br11 0.15. The anions had still large U_{eq} values. This should be results of disordered anions. ISOR instruction was employed to have ellipsoids of sites (All partially occupied Br anions) be restraint to more appropriate values. So, 66 restraints were used for refinement anisotropically.

The checkcif report indicated that structure contains solvent accessible voids of 521.4 Å^3/per unit cell, i.e. some 5.3% of the total volume. Data were also corrected for disordered electron density through use of the SQUEEZE[2] procedure. Attempts to refine peaks of residual electron density as solvent water molecules were unsuccessful. Derived values (formula weight, density, absorption coefficient) do not contain the contribution of the disordered solvent molecule. The residual electron density had a maximum located 1.32 A from atom Br1.

In 7, Fourier maps show that there were severe partial occupancies for all four I$^-$ ions. The occupancies of these sites were freely refined with SUMP instruction firstly, and then the assigned occupancies of many sites were fixed in the process of refinement. The final occupancies of all I$^-$ anions from the refinement were I1A 0.56, I1B 0.36, I1C 0.04, I1D 0.04; I2A 0.70, I2B 0.10, I2C 0.10, I2D 0.10; I3A 0.45, I3B 0.25, I3C 0.18, I3D 0.12; I4A 0.55, I4B 0.15, I4C 0.05, I4D 0.05, I4E 0.05, I4F 0.05, I4G 0.05, I4H 0.05, respectively. With this small occupancy less than 20% it is not worth refining anisotropically for I1C, I1D; I2B, I2C, I2D; I3C, I3D; I4B, I4C, I4D, I4E, I4F, I4G, and I4H. The anions had still large U_{eq} values. This should be results of disordered anions. The checkcif report indicated that structure contains solvent accessible voids of 426.7 Å^3/per unit cell, i.e. some 4.3% of of the total volume. Data were also corrected for disordered electron density through use of the SQUEEZE[2] procedure. Attempts to refine peaks of residual electron density as solvent water molecules were unsuccessful. Derived values (formula weight, density, absorption coefficient) do not contain the contribution of the disordered solvent molecule. The residual electron density had a maximum located 0.63 Å from atom I2D

References

S1. Sheldrick, G. M. (1997). SHELXS97 and SHELXL97. University of Göttingen, Germany.
S2. Spek, A. L. (2003). J. Appl. Cryst. 36, 7-13.